

MonthYear

In-Situ and Ground-Based Intercalibration Measurements of Plasma Density at $L = 2.5$

M. A. Clilverd,¹ F. W. Menk,² G. Milnevski,³ B. R. Sandel,⁴ J. Goldstein,⁵
B. W. Reinisch,⁶ C. R. Wilford,⁷ M. C. Rose,¹ N. R. Thomson,⁸ K. H.
Yearby,⁹ G. J. Bailey,⁷ I. R. Mann,¹⁰ and D. L. Carpenter¹¹

To be submitted to *Journal of Geophysical Research*, January 2003.

G. J. Bailey, Space and Atmosphere Research Group, Department of Applied Mathematics, University of Sheffield, Sheffield, S3 7RH, U.K. (e-mail: G.Bailey@sheffield.ac.uk)

D. L. Carpenter, STAR Laboratory/Electrical Engineering Department, Stanford University, Stanford, California 94305, U.S.A. (e-mail: dlc@nova.stanford.edu)

M. A. Clilverd, British Antarctic Survey, Madingley Road, Cambridge, CB3 0ET, U.K. (e-mail: MACL@bas.ac.uk)

J. Goldstein, Rice University, Rice Space Institute MS-108, 6100 Main Street, Houston, TX 77005-1892, U.S.A. (email: jerru@hydra.rice.edu)

I. R. Mann, Department of Physics, University of York, Heslington, York, YO10 5DD, U.K. (e-mail: ian@aurora.york.ac.uk)

F. W. Menk, School of Mathematical and Physical Sciences and Cooperative Research Centre for Satellite Systems, University of Newcastle, Callaghan, N.S.W., 2308, Australia (e-mail: fred.menk@newcastle.edu.au)

G. Milinevski, Ukrainian Antarctic Center, 16, blvd Tarasa Shevchenka, 01601, Kyiv Ukraine (email: antarc@carrier.kiev.ua)

B. W. Reinisch, Center for Atmospheric Research, University of Massachusetts Lowell, 600 Suffolk Street, Lowell, MA 01854, U.S.A. (e-mail: Bodo_Reinisch@uml.edu)

M. C. Rose, British Antarctic Survey, Madingley Road, Cambridge, CB3 0ET, U.K. (e-mail: MCR@bas.ac.uk)

B. R. Sandel, Lunar and Planetary Laboratory, 1040 East Fourth Street, Room 901, University

of Arizona, Tucson, AZ 85721, U.S.A. (email: sandel@arizona.edu)

N. R. Thomson, Dept. of Physics, University of Otago, Dunedin, New Zealand (email: Thomson@physics.otago.ac.uk)

C. R. Wilford, Space and Atmosphere Research Group, Department of Applied Mathematics, University of Sheffield, Sheffield, S3 7RH, U.K. (e-mail: C.Wilford@sheffield.ac.uk)

K. H. Yearby, Space Instrumentation Group, Department of ACSE, University of Sheffield, Mappin Street, Sheffield, S1 3JD, U.K. (e-mail: K.Yearby@sheffield.ac.uk)

¹British Antarctic Survey, Cambridge, U.K.

²University of Newcastle, Callaghan,
Australia

³Ukrainian Antarctic Center, Kyiv, Ukraine

⁴University of Arizona, Arizona, U.S.A.

⁵Rice University, Houston, Texas, U.S.A.

⁶University of Massachusetts Lowell, Lowell,
U.S.A.

⁷University of Sheffield, Sheffield, U.K.

⁸University of Otago, Dunedin, New Zealand

⁹University of Sheffield, Sheffield, U.K.

¹⁰University of York, York, U.K.

¹¹Stanford University, California, U.S.A.

1. Introduction

It has previously been shown that the plasma number density in the inner magnetosphere can be determined from the interstation phase and amplitude spectra of geomagnetic pulsations between pairs of ground-based magnetometers (*Menk et al.* [1999, 2000]). It is also well known that the plasmaspheric electron number density can be determined by analysing the propagation of ducted man-made whistler-mode signals (*Clilverd et al.* [2000]). Both of these measurements tend to be single point, or at least single longitude. The pulsations are essentially a daytime probe, while the whistler-mode signals are more often observed during nighttime. Good spatial information on the structure of the inner magnetosphere can be obtained using satellite-based experiments, although the measurement repetition rate tends to be low.

The recently launched IMAGE satellite is able to image the structure of the entire plasmasphere (*Sandel et al.* [2000, 2001]). The images are necessarily line-of-sight and require significant interpretation to deconvolve the multi-layered information. Crucially, information on the ion composition of the inner-magnetosphere is necessary to accurately interpret the images during varying periods of geomagnetic activity levels.

Dent et al. [2002] compared magnetometer/VLF/Image RPI measurements made at different latitudes and longitudes for one specific time. In this study we provide the first analysis of data that describes the structure of the inner magnetosphere using all of these techniques, i.e. pulsations, ducted whistler-mode signals, and in-situ satellite measurements, observing the same point on a geomagnetic field-line and at the same longitude. We discuss two representative days and show that the plasma number density results determined from the different techniques are consistent, and can be used to intercalibrate

the EUV Imager images produced by the IMAGE satellite. A coupled plasmasphere-ionosphere model is compared against the observations as a further intercalibration.

2. Experimental Details

2.1. Magnetometer Observations

In order to monitor the plasma mass density at $L=2.5$, we examined ULF geomagnetic field line resonances (FLRs) during January and February 2001 using a combination of ground magnetometer arrays. The primary magnetic data were obtained with an array of 3 Low Powered Magnetometers (LPMs) deployed and operated by the British Antarctic Survey since December 2000 specifically for this project. Fig. 1 shows the locations of these closely-spaced stations located on the Antarctic Peninsula and spanning $2.3 < L < 2.6$ (48°S to 51°S CGM, between -63° and -66° geographic longitude. Their relative locations are indicated by labels M1, M2 and M3.

Fig. 1

Each LPM is an autonomous 3-component fluxgate magnetometer system developed for remote operation in temperatures down to -70°C , in an environment of extreme gales and high static discharge hazard. The systems use GPS timing, solar panels and rechargeable batteries, and conserve power by switching the sensors off between samples. Each system is visited just once per year to download data. The LPM data were sampled in geographic coordinates at 0.1 Hz (averaged from the 5 s measurements) with <1 nT resolution, and rotated into geomagnetic (H, D) coordinates before analysis.

An additional magnetometer at the Ukrainian Antarctic station Vernadsky (50°S CGM; see Fig. 1) provided data from close to the mid-point of two of the LPM systems. This comprises a 3-component LEMI-008 type fluxgate magnetometer that samples the geo-

magnetic field each 1 s with 0.1 nT resolution. This magnetometer has transmitted its data to the British Geological Survey INTERMAGNET project since February 2001.

Additional information on the variation of resonant frequency (and hence mass density) with latitude was obtained using data from the combined SAMNET and BGS magnetometer arrays obtained from the University of York, U.K. For this purpose 5 s measurements with <0.1 nT resolution were examined from 7 SAMNET/BGS magnetometer stations spanning $L=2.24$ to $L=5.47$ between 68° and 79° geomagnetic longitude.

Techniques for the detection of FLRs were summarized by *Menk et al.* [1999] and *Menk et al.* [2000]. When examining data from latitudinally-separated magnetometers, the resonant frequency is identified by the peak in H-component cross-power and cross-phase, and a unity crossing in H-component power ratio, approximately mid-way between the stations. Where only one station is available the resonance is indicated by a peak in the power ratio H/D and a rapid change in polarization i.e., in the phase between the H and D components.

The diurnal pattern of resonance behavior is most clearly seen with dynamic cross-phase spectra [e.g. *Waters et al.* [1991], *Waters et al.* [1995]]. However, all measurements of resonant frequency in this paper were obtained from inspection of discrete FFT cross-power, coherence, power difference, power ratio, and cross-phase spectra on selected days over time windows between 30 and 60 min long, the shorter windows being used under more active conditions.

Mass densities were calculated from the measured resonant frequencies using the analytical expressions described by *Taylor and Walker* [1984] and *Walker et al.* [1992]. These assume decoupled toroidal mode oscillations and yield essentially identical results to the

models described by *Orr and Matthew* [1971]. We used a model distribution of the form R^{-3} , where R is the radial distance in the equatorial plane, since this is where the magnetic field strength and hence Alfvén velocity along a field line generally reach a minimum. This is invalid for very low or high latitude field lines, because of mass loading by ionospheric heavy ions, and field line distortion, but is a satisfactory approximation at $L=2.5$. The choice of power law describing the radial variation in density within the plasmasphere has been discussed by e.g. *Menk et al.* [1999] and *Denton et al.* [2001], although the calculated mass density is relatively insensitive to the actual power law [*Orr and Matthew* [1971]; *Walker et al.* [1992]].

The uncertainty in our calculated mass densities depends mainly on uncertainty in the frequency measurement, and is typically of order 10-15%. We have assumed a dipole magnetic field, and at $L=2.5$ this introduces negligible error. The equatorial mass density can also be determined from comparison of resonance harmonics [*Schulz* [1996]]. That method requires observed frequencies to be accurate to 6% in order to obtain equatorial mass density with a precision of 30% [*Denton and Gallagher* [2000]]. The guided poloidal mode eigenfrequency is $\sim 30\%$ lower than our assumed purely toroidal mode oscillations, so that wave mode coupling may cause the mass density to be slightly underestimated.

2.2. VLF Data

Equatorial electron number densities (N_{eq}) were estimated for $L=2.5$ using man-made VLF whistler-mode signals recorded at Rothera in Antarctica (geographic $67.5^\circ S$, $68.1^\circ W$, $L=2.8$). The VLF Doppler experiment at Rothera receives ducted whistler-mode signals from the east coast U.S. Navy transmitter NAA, 24.0 kHz, 1 MW at Cutler, Maine (geographic $44.6^\circ N$, $67.3^\circ W$, $L=3.0$). Narrowband receivers of the type described by *Thomson*

[1981] are able to separate the whistler mode signals from the stronger subionospheric signal and measure the group delays (t_g), Doppler shifts and arrival bearings of the whistler mode component. Results from these experiments have been published by *Saxton and Smith* [1989], and *Clilverd et al.* [2000].

The method of determining the group delays, L shells and propagation paths of the whistler mode signals was discussed in detail by *Smith and Clilverd* [1991] and *Clilverd et al.* [1991]. The group delay times of the whistler mode signals are determined by cross correlating the plasmaspheric signal with the sub ionospheric signal, accumulating the coefficients for 15 minutes at a time. The L shell has in the past been determined by measuring the difference in group delay time for two different transmitter frequencies traveling in the same duct. The time difference is due to dispersion along the field line and is dependent on the L shell of propagation. In this study we use the simplification that the average group delay observed is representative of equatorial electron number density conditions at $L=2.5$. The error incurred by using this simplification is $\sim 0.1 L$. As the longitude of the transmitter and the receiver are so similar the whistler-mode signals exit the ionosphere close to the Antarctic Peninsula LPM array. The intercomparison between this technique and FLRs has been discussed by *Menk et al.* [1999] and *Dent et al.* [2002].

2.3. IMAGE Satellite Data

The IMAGE spacecraft is in an elliptical polar orbit with an apogee altitude of 7.2 Earth radii (46,000 km) and a perigee altitude of 1,000 km, and completes one orbit every 14.2 hours. This study presents data from 2 of the 7 instruments on board the spacecraft. The RPI experiment provides the electron number density as IMAGE transits through

the plasmasphere, and the EUV Imager experiment images geospace using He^+ emissions when the spacecraft is near apogee looking back towards the Earth.

The RPI instrument (*Reinisch et al.* [2000], *Carpenter* [2002]) is a low-power radar which operates in the radio frequency bands which contain the plasma resonance frequencies characteristic of the Earth's magnetosphere (3 kHz to 3 MHz). In the passive receive-only mode, RPI receives the natural plasma wave emissions from 3 kHz to 1.1 MHz, using these to determine the electron number density to within an accuracy of 10%. In this study we are able to make use of the fact that the orbit of IMAGE takes it close to the geomagnetic equator at $\sim L=2.5$, so that there is no adjustment to make in order to compare the RPI measurements with the VLF Doppler electron number density estimates.

The Extreme Ultraviolet Imager (EUV Imager) images the distribution of He^+ in Earth's plasmasphere by detecting its resonantly-scattered emission at 30.4 nm (*Sandel et al.* [2001]). Effective imaging of the plasmaspheric He^+ requires global 'snapshots' in which the high apogee and the wide field of view of the EUV Imager provide in a single exposure a map of the entire plasmasphere. The 30.4 nm feature is relatively easy to measure because it is the brightest ion emission from the plasmasphere, it is spectrally isolated, and the background at that wavelength is negligible. Line-of-sight measurements are easy to interpret because the plasmaspheric He^+ emission is optically thin, so its brightness is directly proportional to the He^+ column abundance. The EUV Imager instrument consists of three identical sensor heads, each having a field of view of 30° . These sensors are tilted relative to one another to cover a fan-shaped field of $84^\circ \times 30^\circ$, which is swept across the plasmasphere by the spin of the satellite. EUV Imager's spatial resolution is $\sim 0.6^\circ$ or $\sim 0.1 R_E$ in the equatorial plane seen from apogee. The sensitivity

is sufficient to map the position of the plasmapause with a time resolution of 10 minutes or better.

2.4. Plasmasphere-Ionosphere Model

We compare the measured densities with modeled values of electron and ion number densities in the equatorial region of the $L=2.5$ field-line. These have been determined from SUPIM, the Sheffield University Plasmasphere Ionosphere Model [Bailey and Sellek [1990]; Bailey *et al.* [1993]; Bailey and Balan [1996]]. In SUPIM, coupled time-dependent equations of continuity, momentum, and energy balance are solved along closed magnetic field lines between altitudes of around 120 km in conjugate hemispheres for the concentrations, field-aligned fluxes, and temperatures of the O^+ , H^+ , He^+ , N_2^+ , O_2^+ , and NO^+ ions and the electrons. For the present study, the geomagnetic field is represented by an eccentric dipole. The concentrations and temperatures of the neutral gases are obtained from the MSIS86 thermospheric model [Hedin, 1987], the neutral wind velocities from the HWM90 neutral wind model [Hedin *et al.*, 1991], and the solar EUV fluxes from the EUVAC solar EUV flux model of Richards *et al.* [1994]. The remaining model inputs, such as the photoionization and photoabsorption cross sections, the chemical reaction rates, the heating and cooling rates, and the collision frequencies, are described in Bailey and Sellek [1990], Bailey *et al.* [1993], and Bailey and Balan [1996].

3. Results

3.1. Overview

The low-power magnetometers were deployed in Antarctica and commenced data recording in December 2000, and have operated continuously since then. The VLF Doppler

experiment has been operating concurrently. This paper presents results from two days of data from the first summer of operation, through to early March 2001. Geomagnetic conditions during this time were relatively quiet, with no significant magnetic storms. The two days selected for detailed study, January 22 and February 14 2001, are two of the more disturbed periods during this time, when the occurrence of ducted VLF signals and ULF pulsation activity is likely to peak. To assess this we examined: (i) monthly scatter plots of the group delay of NAA VLF Doppler signals received at Rothera, (ii) monthly scatter plots of the local time distribution of these Doppler signals, and (iii) time series records from the co-located magnetometers.

On the first day examined, January 22, K_p reached 4– after peaking the previous day at 4₀. A_p reached 19 on January 21, again indicative of moderately disturbed conditions, while the previous 10 days had registered a maximum of only 9. The maximum K_p on the second selected day, February 14, was again 4–, after peaking at 5– just before midnight on February 13. A_p reached 25 on February 13, again indicative of moderately disturbed conditions, while the previous 10 days had registered a maximum of 14 on February 6. The sunspot number on January 22 was 93 while for February 14 it was 68. Thus both selected days represent moderately disturbed conditions, occurring after an extended quiet period.

The RPI electron number density data can also provide information on the state of the plasmasphere during these days. Fig. 2 shows the scaled plasma wave results for passes through the plasmasphere made at about 08–11 UT on both study days (dotted and dash-dot lines), pulsation FLR results from the U.K. SAMNET array (solid lines), and the empirical model results of Carpenter and Anderson [1992](dashed lines). The

Fig. 2

RPI results include extrapolations from the point of measurement to the geomagnetic equatorial plane at each L -shell. This done by simply assuming the density along a field line is uniform over the small range of L -shells considered here where the satellite is close to the geomagnetic equator (*Goldstein et al.* [2001]). Also included in the figures are mass densities and electron densities derived from the LPs and VLF experiments near $L=2.5$ on the Antarctic Peninsula (open circles and filled triangles respectively). For the January 22 plot uncertainty in the ULF-derived mass density is indicated by error bars. For clarity these have not been shown in the February 14 plot, although the uncertainties are similar.

The January 22 data (top panel) are best represented by an extended plasmapause about $0.5 L$ wide situated somewhere near $L=3.8$. The IMAGE spacecraft pass is from 8.04-8.76 UT and 4.64-5.04 MLT. The model and RPI electron densities are similar around $L=2.5$ - 3.3 even though there is little overall agreement throughout the plasmasphere. Beyond $L=4.3$ the RPI density extrapolations become unreliable as the spacecraft ascends to $>20^\circ$ latitude above the equatorial plane.

The plasma mass density (solid line) was determined between 0800-0840 UT for a range of L -values using SAMNET and BGS magnetometer data at about 0° longitude. There is good overall agreement between the RPI experiment and the mass density values, although the mass densities tend to be slightly lower. This is primarily because of the influence, at this time of year, of the longitudinal amplitude of the annual variation in plasmaspheric electron number densities (*Ciliverd et al.* [1991]). At longitudes of the Antarctic Peninsula (60 – 70° W geographic), high concentrations of electrons would be expected in January compared with those in June, while at the longitudes of Europe, Africa and India such

high concentrations would not be expected in January. This effect tends to counteract the influence of heavy ions on the observed ion mass densities, which would normally result in higher ion mass densities than electrons concentrations at the same location. Higher ion mass densities (circle) and electron concentrations (solid triangle) at longitudes of the Antarctic Peninsula at this time of year are confirmed at $L=2.5$ by the experimental observations discussed in this paper.

On February 14 (bottom panel) a reasonably well-defined plasmopause is present in the IMAGE RPI measurements. Data from two orbits are shown in the figure: 9.01-10.31 UT (15.28-15.08 MLT; dotted line), and 11.01-11.57 UT (3.49-2.93 MLT; dot-dash line). The plasmopause location is around $L=2.97$ -3.12 and $L=3.22$ -3.5 during these passes. Ion mass density data determined from the SAMNET/BGS magnetometer array are also shown for two times: 0600-0650 UT (solid line) and 0800-0850 UT (heavy line). There are significant differences in the shape and position of the plasmopause derived from the measurements at these times. This suggests that there are temporal and longitudinal variations in both electron density and heavy ion concentration during this day.

Again, the $L=2.5$ ion mass density and electron density measurements are somewhat higher than values at other longitudes. Note that at $L < 2.7$ the ion mass densities are also significantly higher than the RPI and model electron densities.

Clearly, when comparing the results from a range of instruments it is important to consider their relative locations. This paper uses data from longitudes in the Antarctic Peninsula region. On January 22, 2001 IMAGE passes the geomagnetic equator near $L=2.5$ between 290–310 ° E. Thus the ground-based and satellite measurements are closely co-located. On February 14, 2001 IMAGE passes the geomagnetic equator near $L=2.5$

at about 240 ° E (geographic), or 50 ° west of the Antarctic Peninsula region where the ground-based measurements are made. Although still in the same longitudinal region in terms of the likely influence of the annual variation in plasma density at $L=2.5$ the difference may still be significant as further analysis shows.

3.2. January 22, 2001

The ground-based Antarctic Peninsula magnetometer data come from a region centered on the Ukrainian Station of Vernadsky. The determination of the magnetospheric plasma mass density distribution is dependent on the presence of field-line resonances in the ULF data. Representative magnetometer time series from 06:00–12:00 UT from Vernadsky are shown in Fig. 3, where 6 one hour sections of data are stacked vertically. The amplitude scale is 2 nT and is shown on the left hand y-axis. The plot shows that small but discernable pulsations occur at most times, allowing good UT coverage for the mass density analysis. This is expected for moderately disturbed geomagnetic conditions and was a primary influence on the dates selected in this study.

Fig. 3

The diurnal variation in magnetospheric plasma mass density near the equatorial plane at $L=2.5$ on January 22, 2001 is shown by the open circles with error bars in Fig. 4. The average mass density is close to 3000 amu cm⁻³ for most of the day, although slightly lower values occur during the nighttime hours before 0800 UT (04 LT). Reasonable data coverage extends until around 17 UT when pulsation activity became weaker. Also shown on Fig. 4 are the electron number densities, derived by both the VLF Doppler experiment (filled triangles with error bars) and the RPI experiment (filled squares with error bars). These show a near 1:1 correlation with the mass densities.

Fig. 4

Fig. 4 also shows results from the SUPIM model at the geomagnetic equator of the $L=2.5$ field-line based on the solar and geomagnetic conditions for this day. The model starts from arbitrary initial conditions and then runs for several calculation days until the output values converge. The dashed line indicates the diurnal variation of the model electron number density, which shows good agreement with the equivalent VLF values during the nighttime (00–07 UT). The solid line indicates the plasma mass density, which also shows reasonable agreement with the ULF observations during the first third of the day, and a similar diurnal range. However, the phase of the model variation is offset from that of the observations by 4–5 hours. The difference between the model electron density and model mass density results is due to the presence of heavy ion populations in the model. During the day the proportion of He^+ to H^+ in the model is about 2.6% by number and 10.5% by mass, while O^+ increases from 0.7% to 1.0% by number or 11–16% by mass.

Fig. 5 is an EUV Imager image from January 22, 2001. It is the sum of 8 individual EUV Imager images that have been rebinned in L -shell and magnetic longitude space (*Sandel et al.* [2003]) and then added. Thus the brightness of this image represents the He^+ distribution in the plane of the magnetic equator. The innermost white circle corresponds to the solid Earth. Auroral emission is present about half-way from the center to the Earth’s limb between magnetic longitudes of approximately 0 and 180°. Earth’s shadow moves in magnetic longitude, so it is smeared by summing the rebinned images. The position of the field-line at $L=2.5$, magnetic longitude = 10°E (shown by the white circle to the right of the Earth) is outside the shadow for all the images used in this work, so our determination of He^+ column abundances is not compromised. We used this type of

Fig. 5

plot to determine the line-of-sight He^+ abundance for the line of sight at the white circle, and found a value of $5.8 \times 10^{10} \text{ cm}^{-2}$.

3.3. February 14, 2001

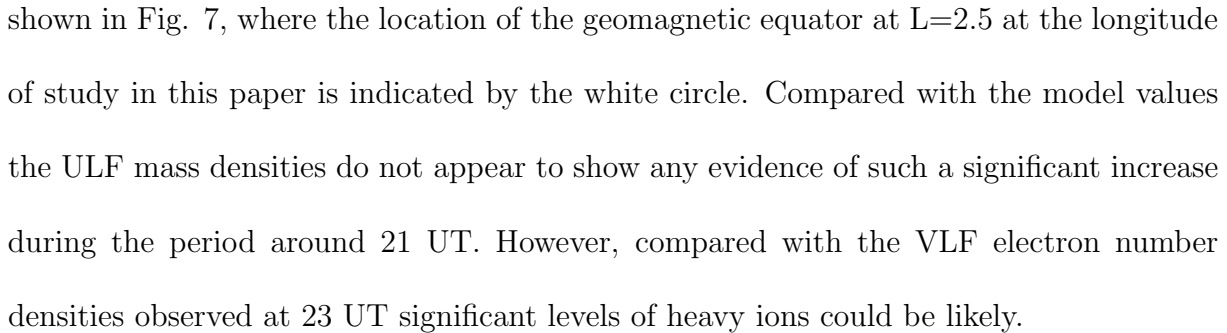
The magnetospheric plasma mass density distribution near $L=2.5$ on February 14, 2001 is represented by the open circles in Fig. 6. The plot format is the same as Fig. 4 for January 22. It is noticeable, however, that on February 14 the mass densities are somewhat higher, at about $4500 \text{ a.m.u. cm}^{-3}$, but the electron number densities determined from the VLF Doppler experiment still track the mass densities. However, the RPI ‘snapshot’ values (2200 el. cm^{-3}) are significantly lower, by a factor of 2 around 10 UT. As mentioned previously near 09 UT and 11 UT the IMAGE satellite was respectively about 150° east and 50° west of the ground stations, and this may be why the in situ observations are significantly different from the other experiments. Analysis of naturally occurring whistlers propagating at about 320°E geographic longitude confirms electron number densities of 4000 el. cm^{-3} at $L=2.5$, while estimates from a second VLF Doppler system in Dunedin, New Zealand (*Thomson* [1981]) also agree with the high electron values observed on this day.

Fig. 6

Fig. 6 also shows results from the SUPIM model at the geomagnetic equator of the $L=2.5$ field line based on the solar and geomagnetic conditions for this day. The dashed line again indicates the diurnal variation of the model electron number density, which shows good agreement with the equivalent VLF values at night. The solid line indicates the plasma mass density, which also shows good agreement with the ULF observations, especially during the first half of the day. A significant difference between this model run and the one undertaken for January 22, 2001, above is that the photoionization rate used

for February 14 was twice as large and consequently all the density results are higher throughout the day. The photoionization rate used on this day was typical for standard model runs, while those for January 22 represent lower than normal rates. The percentage of He^+ to H^+ in the model for February 14 is again about 2.6% by number and 10.5% by mass, while O^+ increases throughout the day from 0.7% to 1.0% by number or 11–16% by mass.

The EUV Imager data for February 14 were analysed when IMAGE was close to apogee on 2 orbits. The first measurements at $L=2.5$ were made between 23:44 (the previous day)–01:26 UT and gave an average column abundance of $6.7 \times 10^{10} \text{ cm}^{-2}$. The second period was during 21:42–22:13 UT where the column abundance was $11.0 \times 10^{10} \text{ cm}^{-2}$. This second period appears to be associated with a tongue of more intense He^+ emission as shown in Fig. 7, where the location of the geomagnetic equator at $L=2.5$ at the longitude of study in this paper is indicated by the white circle. Compared with the model values the ULF mass densities do not appear to show any evidence of such a significant increase during the period around 21 UT. However, compared with the VLF electron number densities observed at 23 UT significant levels of heavy ions could be likely.


Fig. 7

4. Discussion

In previous studies of the ion and electron structure of the plasmasphere *Menk et al.* [1999] and *Menk et al.* [2002] used spatially separated measurements, correcting for local time effects in order to inter-compare the results. In this study we show the advantage of using co-located instruments in that no corrections need to be made in order to compare the results.

Here we have chosen two days with similar geomagnetic conditions, where the IMAGE satellite passed close to the equatorial region of an $L=2.5$ field-line connecting to a cluster of ground-based experiments measuring similar parameters. While the two study days seem to relate to similar conditions within the inner plasmasphere, the outer plasmasphere is quite different on the two days, with more structure and a well defined plasmapause present on February 14, 2001. This may be due to different solar wind conditions. The solar wind speed was almost constant around 320 km s^{-1} over most of January 20-21, 2001, reaching a plateau around 500 km s^{-1} on January 22. The solar wind speed was in the range $400\text{-}450 \text{ km s}^{-1}$ on 12 February, but in the range $480\text{-}610 \text{ km s}^{-1}$ on February 13 and 14. The solar wind proton density was between 2 and 20 cm^{-3} over January 20-22, with a short large increase to 60 cm^{-3} late on January 21. Over February 12-13 the solar wind proton density was generally between $5\text{-}10 \text{ cm}^{-3}$, and $<6 \text{ cm}^{-3}$ on February 14. Thus solar wind pressure (which is proportional to nV^2) was significantly higher over February 12-13 than over January 20-21. This may also explain why double the photoionization rates were required in the SUPIM model to reproduce the ground-based observations on February 14 compared to January 20. The IMF B_z component was similar during both January 20-21 and February 12-13, with positive variations and several excursions to below -7 nT .

Using the EUV Imager experiment on IMAGE we find that the column abundance of He^+ changed from 5.8 to $6.7 \times 10^{10} \text{ cm}^{-2}$ between January 22 to February 14. This is in qualitative agreement with the observed change in general plasma concentration between the two days. More generally it appears that a typical value of $6 \times 10^{10} \text{ cm}^{-2}$ is appropriate for comparison with the ground-base observations. We used this value to investigate the

unexpectedly lower electron number density values on February 14 when IMAGE was 50° west of the ground stations. EUV Imager values from that region made at 13–14 UT indicate column abundances of only $3.6 \times 10^{10} \text{ cm}^{-2}$, which is suggestive of a region of plasma depletion that may have been present during this period and that could explain the IMAGE RPI values determined only 3 hours earlier.

The ratio of He^+ to H^+ ions in the plasmasphere can be described from an empirical expression given by *Craven et al.* [1997]. The ratio decreases with radial distance and depends on the solar activity 10.7 cm flux. At $L=2.5$ the typical mass ratio of $\text{He}^+:\text{H}^+$ is about 0.1, with a range from 0.03–0.3. The solar flux measure F10.7 was typically about 150 during January/February, which *Craven et al.* [1997] suggests should result in the abundance of $\text{He}^+:\text{H}^+$ being 10% at $L=2.5$. Using the values of electron number density and ion mass density from 04:00 UT on January 22, 2001, and assuming charge neutrality, we find that He^+ is about 3.8% of the abundance of H^+ . Similar constraints on the values determined from 08:00 UT on February 14, 2001, when the electron number density is generally higher on this day than on January 22 (4000 el cm^{-3} compared with 3000 el cm^{-3}), gives He^+ abundance levels of about 3.3% by number and about 13–14% by mass. However, the estimated number density of He^+ atoms actually increases from 110 to 130 cm^{-3} , or a ratio of about 1.2. From the EUV Imager images we know that the abundance of He^+ on the first half of these two days also shows a similar increase ($6.7/5.8=1.2$).

Having determined the typical column abundance figure for $L=2.5$ can we relate this to the concentration values that we find in the equatorial region? Modelling shows that the measured radial profiles of He^+ column density near $L=2.5$ are similar in shape to those computed by integrating the RPI electron density profiles such as those shown in

Fig. 2 (*Sandel et al.* [2003]). This implies that we can take the L -dependence for He^+ near $L=2.5$ to be the same as that measured for electrons by RPI. We can then use the profiles of electron density measured by RPI to compute an effective path length (P). Here P is the length of the column of He^+ having uniform density equal to the region of maximum i.e., equatorial, density along the line of sight, and having the measured column density. For the plasma distributions seen near $L=2.5$, we find $P=1.8$ Re. Then the measured column density corresponds to an equatorial concentration of $52 \text{ He}^+ \text{ cm}^{-3}$ in this region. With H^+ levels close to the electron number density of about 3000 el. cm^{-3} we find that this would result in He^+ occurrence levels of 1.7% by number and 6.9% by mass. As the VLF and ULF measurements are biased to about 10% of the length of the magnetic field line that lies near the equatorial plane ($0.5 R_E$ for an $L=2.5$ field-line) we could probably multiply the above intercomparison result by a factor of 2 to allow for the difference in effective path length i.e., 1.8 Re to 0.5 Re. As a result we might expect about 3-4% He^+ by number and 10-15% by mass from these calculations. Although modeling will be required to complete this picture in detail it does appear that this simple calculation confirms the analysis made from the ground-based observations.

At 22:00 UT on February 14 the IMAGE EUV Imager measurements suggest that the abundance of He^+ exceeded the values that were observed on January 22 by almost a factor of 2 i.e., 11 instead of $6 \times 10^{10} \text{ cm}^{-2}$. Although data on the electron number densities are sparse at this time, the disparity between the ULF mass densities and the VLF electron number densities between 20–23 UT shown in Fig. 6 suggests that heavy ions must be an influence. Once again requiring charge neutrality we find that the 20–23 UT observations are consistent with He^+ being about 8% of H^+ by number, with the

actual levels being about 250 cm^{-3} . As a ratio of the values earlier in the day this is $250/130=1.9$, which compares well with the ratio of the equivalent column abundances i.e., $11/6.7=1.6$. A near doubling of just He^+ in the tongue of emission visible at 21 UT would be enough to produce the majority of the change in mass density levels to above $4000 \text{ a.m.u cm}^{-3}$ observed at about 21 UT.

With this confidence in inter-comparing the EUV Imager and ground-based experiments we can now consider the relevance of the EUV Imager observations made at the location where the RPI measurements were significantly lower than the ground station observations on February 14. EUV Imager levels of $3.6 \times 10^{10} \text{ cm}^{-2}$ are a factor of about $3.6/6.7=0.53$ down on the Antarctic Peninsula values. As we estimated that electron number densities there were 4000 el. cm^{-3} we would estimate RPI values of 2150 el. cm^{-3} to the west. Clearly, this value equates well to the observed RPI value of 2200 el. cm^{-3} and confirms the presence of significant depletion structures in the plasmasphere on this day.

5. Conclusions

Using two ground-based experiments and two satellite-borne experiments we have been able to interpret changes in plasmaspheric composition at the same point in space during moderate geomagnetic activity. We have analysed data from January 22, 2001 and February 14, 2001 on an $L=2.5$ magnetic field line at the longitude of the Antarctic Peninsula. Mass density was determined from an array of magnetometers, while the electron number density was determined from analysis of the group delay of man-made VLF transmissions from north east America. The IMAGE satellite RPI experiment provided in-situ plasma wave measurements of the electron number density in the equatorial region of the $L=2.5$

field line, while a few hours later the IMAGE EUV Imager experiment was able to resolve the He^+ abundance by looking back toward the same spot.

On January 22, 2001 the mass density and electron number density were very similar all day. The levels were consistent with a moderately-disturbed plasmasphere. The electron number density from IMAGE RPI was also in good agreement with the ground-based measurements at the times when it was close to the equatorial region of the $L=2.5$ field line. The IMAGE EUV Imager measurements of He^+ were relatively uniform throughout the plasmasphere, again indicative of moderately-disturbed conditions, and the column abundance value of $5.8 \times 10^{10} \text{ cm}^{-2}$ is taken to represent those conditions. There was about 4% by number and 16% by mass of He^+ relative to H^+ at this time. On February 14, 2001 there appeared to be significantly more response of the plasmasphere to the moderate ($K_p=5$) activity levels. The electron number density and the mass density showed a significant increase compared with January 22 for most of the day. The IMAGE EUV Imager experiment also indicated that a 20% increase in the abundance of He^+ could be seen between these two days.

We find that for the longitudes of the Antarctic Peninsula, and therefore the Americas, an EUV Imager He^+ column abundance value of $6 \times 10^{10} \text{ cm}^{-2}$ is equivalent to plasmaspheric electron density levels of 3000 cm^{-3} at $L=2.5$. We also find that for these conditions the He^+ mass abundance is about 12-16% compared with H^+ . Both decreases and increases in the He^+ column abundance are appear to be linearly correlated to changes in the percentage occurrence of He^+ as determined from a combination of ground-based VLF and ULF observations, as well as in-situ measurements from the RPI experiment.

Acknowledgments. The Antarctic field work was carried out under the auspices of the NERC Antarctic Funding Initiative (AFI) with logistic support from the British Antarctic Survey. Aspects of this work were supported by the Australian Research Council, the CRC for Satellite Systems, and the University of Newcastle.

References

- Bailey, G.J., and R. Selleck, A mathematical-model of the Earths plasmasphere and its application in a study of He^+ at $L=3$, *Ann. Geophys.*, *8*, 171–189, 1990.
- Bailey, G.J., R. Selleck, Y. Rippeth, A modelling study of the equatorial topside ionosphere, *Ann. Geophys.*, *11*, 263–272, 1993.
- Bailey, G.J., and N. Balan, Some modelling studies of the equatorial ionosphere using the Sheffield University Plasmasphere Ionosphere Model, *Adv. Space Res.*, *18*, 59–68, 1995.
- Carpenter, D.L., M. A. Spasojevic, T. F. Bell, U. S. Inan, B. W. Reinisch, I. A. Galkin, R. F. Benson, J. L. Green, S. F. Fung, and S. A. Boardsen, Small-scale field-aligned plasmaspheric density structures inferred from the Radio Plasma Imager on IMAGE, *J. Geophys. Res.*, *107*, 1258, doi:10.1029/2001JA009199, 2002.
- Carpenter, D.L., and R.R. Anderson, An ISEE/whistler model of equatorial electron-density in the magnetosphere, *J. Geophys. Res.*, *97*, 1097–1108, 1992.
- Clilverd, M. A., A. J. Smith, and N. R. Thomson, The annual variation in quiet time plasmaspheric electron density determined from whistler mode group delays, *Planet. Space Sci.*, *39*, 1059–1067, 1991.
- Clilverd, M. A., B. Jenkins, and N. R. Thomson, Plasmaspheric storm time erosion, *J. Geophys. Res.*, *105*, 12997–13008, 2000.

- Craven, P. D., D. L. Gallagher, and R. H. Comfort, Relative concentration of He^+ in the inner magnetosphere as observed by the DE 1 retarding ion mass spectrometer, *J. Geophys. Res.*, *102*, 2279–2289, 1997.
- Dent, Z.C., I.R. Mann, F.W. Menk, J. Goldstein, C.R. Wilford, M.A. Clilverd, and L.G. Ozeke, A coordinated ground-based and IMAGE satellite study of quiet-time plasmaspheric density profiles, *Geophys. Res. Lett.*, Submitted, 2002.
- Denton, R.E., M.R. Lessard, R.R. Anderson, E.G. Miftakhova, and J.W. Hughes, Determining the mass density along magnetic field lines from toroidal eigenfrequencies: Polynomial expansion applied to CRRES data, *J. Geophys. Res.*, *106*, 29915–29924, 2001.
- Denton, R. E., and D. L. Gallagher, Determining the mass density along magnetic field lines from toroidal eigenfrequencies, *J. Geophys. Res.*, *105*, 27717–27725, 2000.
- Goldstein, J., R. E. Denton, M. K. Hudson, E. G. Miftakhova, S. L. Young, J. D. Menietti, and D. L. Gallagher, Latitudinal density dependence of magnetic field lines inferred from Polar plasma wave data, *J. Geophys. Res.*, *106*, 6195–6201, 2001.
- Menk, F. W., D. Orr, M. A. Clilverd, A. J. Smith, C. L. Waters, and B. J. Fraser, Monitoring spatial and temporal variations in the dayside plasmasphere using geomagnetic field line resonances, *J. Geophys. Res.*, *104*, 19955–19970, 1999.
- Menk, F. W., C. L. Waters, and B. J. Fraser, Field line resonances and waveguide modes at low latitudes, 1. Observations, *J. Geophys. Res.*, *105*, 7747–7761, 2000.
- Menk, F. W., I. R. Mann, A. J. Smith, C. L. Waters, M. A. Clilverd, and D. K. Milling, Monitoring the plasmapause using geomagnetic pulsations. 1. Field line resonances, *J. Geophys. Res.*, submitted, 2002.

- Orr, D., and J. A. D. Matthew, The variation of geomagnetic micropulsation periods with latitude and the plasmopause, *Planet. Space Sci.*, *19*, 897–904, 1971.
- Reinisch, B.W., D. M. Haines, K. Bibl, G. Cheney, I.A. Galkin, X. Huang, S.H. Myers, G.S. Sales, R.F. Benson, S.F. Fung, J.L. Green, S. Boardsen, W.W.L. Taylor, J.-L. Bougeret, R. Manning, N. Meyer-Vernet, M. Moncuquet, D.L. Carpenter, D.L. Gallagher, and P. Reiff, The radio plasma imager investigation on the IMAGE spacecraft, *Space Sci. Rev.*, *91*, 319–359, 2000.
- Sandel B.R., A.L. Broadfoot, C.C. Curtis, R.A. King, T.C. Stone, R.H. Hill, J. Chen, O.H.W. Siegmund, R. Raffanti, D.D. Allred, R.S. Turley, and D.L. Gallagher, The extreme ultraviolet imager investigation for the IMAGE mission, *Space Sci. Rev.*, *91*, 197–242, 2000.
- Sandel B.R., J. Goldstein, D.L. Gallagher, and M. Spasojevic, Extreme ultraviolet imager observations of the structure and dynamics of the plasmasphere, *Space Sci. Rev.*, In Press, 2003.
- Sandel B.R., R.A. King, W.T. Forrester, D.L. Gallagher, A. L. Broadfoot, C.C. Curtis, Initial results from the IMAGE extreme ultraviolet imager, *Geophys. Res. Lett.*, *28*, 1439–1442, 2001.
- Saxton, J. M., and A. J. Smith, Quiet time plasmaspheric electric fields and plasmasphere-ionosphere coupling fluxes at $L = 2.5$, *Planet. Space Sci.*, *37*, 283–293, 1989.
- Schulz, M., Eigenfrequencies of geomagnetic field lines and implications for plasma-density modeling, *J. Geophys. Res.*, *101*, 17385–17397, 1996.
- Smith, A. J., and M. A. Clilverd, Magnetic storm effects on the mid-latitude plasmasphere, *Planet. Space Sci.*, *39*, 1069–1079, 1991.

- Taylor, J. P. H., and A. D. M. Walker, Accurate approximate formulae for toroidal standing hydromagnetic oscillations in a dipolar geomagnetic field, *Planet. Space Sci.*, *32*, 1119–1124, 1984.
- Thomson, N. R., Whister mode signals - spectrographic group delays, *J. Geophys. Res.*, *86*, 4795–4802, 1981.
- Walker, A. D. M., J. M. Ruohoniemi, K. B. Baker, R. A. Greenwald, and J. C. Samson, Spatial and temporal behaviour of ULF pulsations observed by the Goose Bay HF radar, *J. Geophys. Res.*, *97*, 12187–12202, 1992.
- Waters, C. L., F. W. Menk, and B. J. Fraser, The resonance structure of low latitude Pc3 geomagnetic pulsations, *Geophys. Res. Lett.*, *18*, 2293–2296, 1991.
- Waters, C. L., J. C. Samson, and E. F. Donovan, The temporal variation of the frequency of high latitude field line resonances, *J. Geophys. Res.*, *100*, 7987–7996, 1995.

Figure 1. Map of the Antarctic Peninsula showing the positions of the low power magnetometer sites (M1, M2, M3), Vernadsky magnetometer (diamond), the VLF Doppler receiver site (asterisk), and the typical field line footprint of study (cross).

Figure 2. Variation of plasma density through the magnetosphere near 10 UT on January 22 (top panel) and February 14, 2001 (bottom panel). IMAGE RPI electron densities are indicated by the dotted line (08:00 UT on January 22 and 09:00 UT on February 14) and dash-dot line (11:00 UT on February 14). Ion mass densities determined using the SAMNET/BGS magnetometer arrays are denoted by the solid line (08:00-08:50 UT on January 22 and 06:00-06:50 UT on February 14) and heavy solid line (08:00-08:50 UT on February 14). The dashed line in both plots represents the empirical model of Carpenter and Anderson for these geomagnetic conditions. Finally, open circles and solid triangles indicate $L=2.5$ ion mass density and electron density at the Antarctic Peninsula.

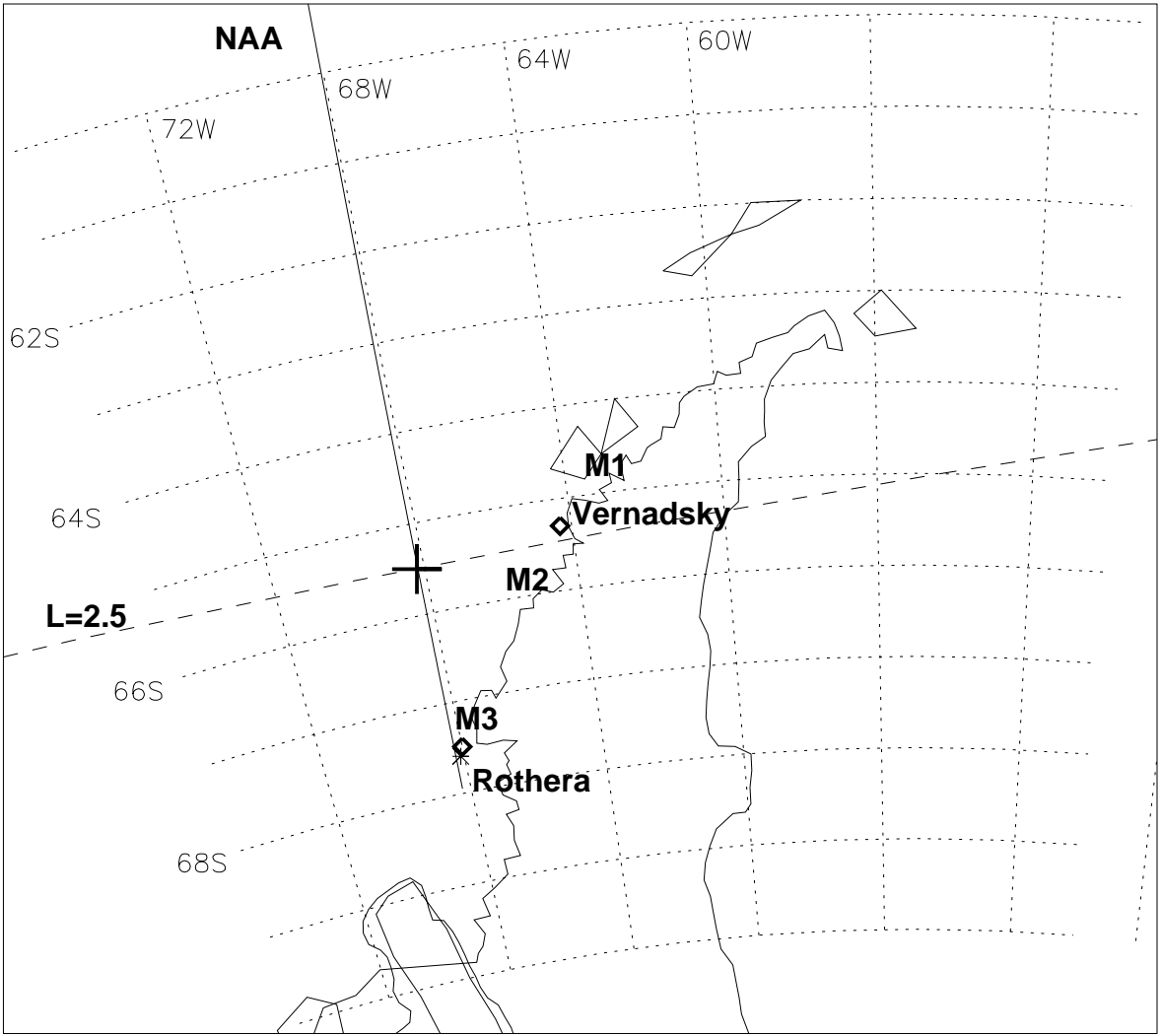
Figure 3. An example of the Vernadsky magnetometer data on January 22, 06:00–12:00 UT, showing small pulsations of about 1 nT amplitude.

Figure 4. Ion mass density (open circles) and electron density (triangles) variations on January 22, 2001. SUPIM model results for electron number density (dashed line) and ion mass density (solid line) are shown for comparison. RPI electron number density values are given by the solid squares. Error estimates for each observation are indicated by the vertical lines and are typically 10%.

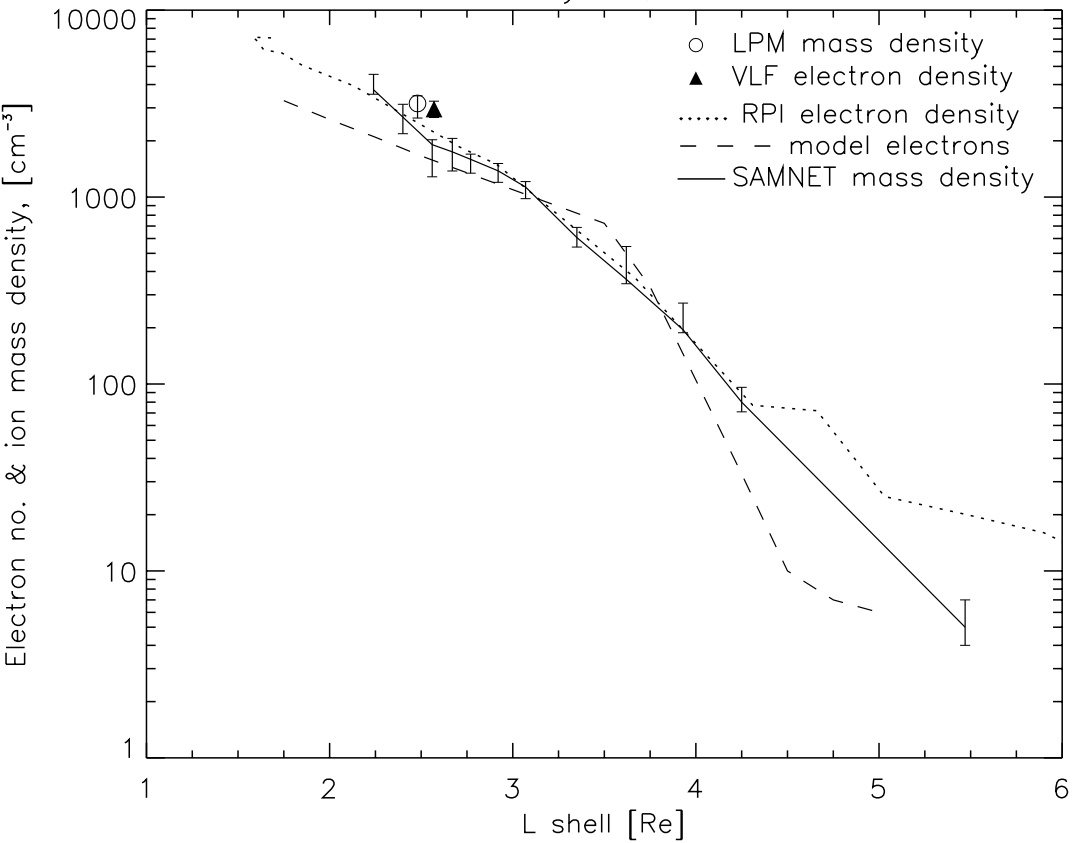
Figure 5. EUV Imager view of the near-Earth environment on January 22, 2001. This composite includes 8 individual EUV images acquired from 00:51 to 02:02 UT, when IMAGE was at magnetic latitudes from 77°N to 68°N and radial distances from 8.11 to 7.90 Re. The image is projected into the plane of the magnetic equator, and the white grid shows L and magnetic longitude, with 0° magnetic longitude to the right. The white circle is at the position of the Antarctic Peninsula $L=2.5$ field-line. The dark mask over the lower parts of the image marks regions of incomplete coverage or scattered sunlight.

Figure 6. Ion mass density and electron density on February 14, 2001, in the same format as Fig. 4.

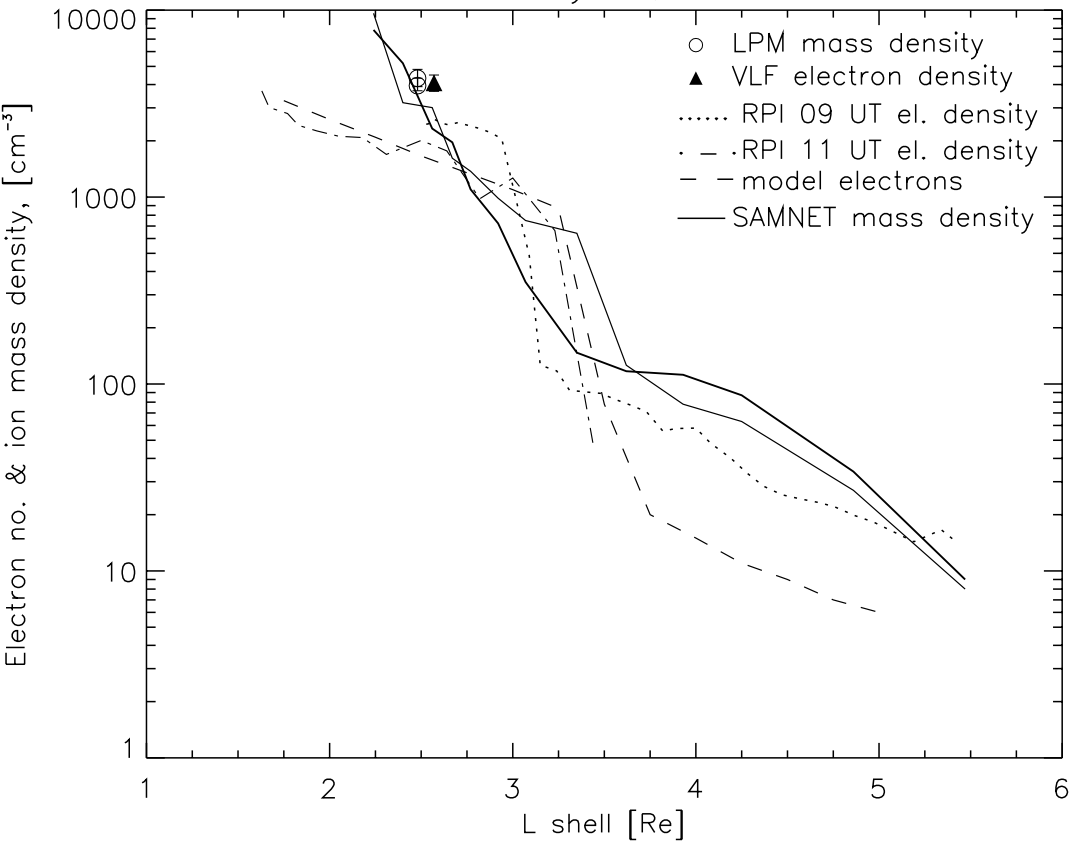
Figure 7. EUV Imager view of the near-Earth environment at 21:45 UT on February 14, 2001. This composite includes 4 individual EUV images acquired from 21:42 to 22:13 UT, when IMAGE was at magnetic latitudes from 61°N to 56°N and radial distances from 6.44 to 5.92 Re. The presentation is the same as in Fig. 5.



January 22, 2001



February 14, 2001



VERNADSKY H COMPONENT TIME SERIES
22 JANUARY 2001 ($5 < f < 30$ mHz)

